UNIVERSITY
OF BERN

X-ray microtomography

485018-HS2024-0: Advanced Course II Ultraprecision Engineering

David Haberthür
Institute of Anatomy, September 25, 2024

Grüessech mitenang!

- David Haberthür
  - Physicist by trade
  - PhD in high resolution imaging of the lung, Institute of Anatomy, University of Bern, Switzerland
  - Post-Doc I: TOMCAT, Swiss Light Source, Paul Scherrer Institute, Switzerland
  - Post-Doc II: µCT group, Institute of Anatomy, University of Bern, Switzerland.

Grüessech from the µCT group

David.Haberthuer@unibe.ch Ruslan.Hlushchuk@unibe.ch Oleksiy.Khoma@unibe.ch

µCT-group

- microangioCT [1]
  - Angiogenesis: heart, musculature [2] and bones
  - Vasculature: (mouse) brain [3], (human) nerve scaffolds [4], (human) skin flaps [5] and tumors
- Zebrafish musculature and gills [6]
- (Lung) tumor detection and metastasis classification [7]
- Collaborations with museums [8] and scientist at UniBe [9] to scan a wide range of specimens
- Automate *all* the things! [10], [11]

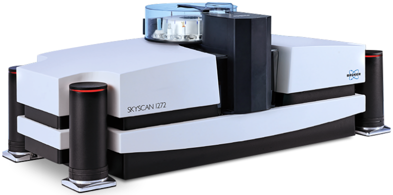

bruker.com/skyscan1272

Contents

µCT

- Dense and/or non-transparent samples
- Calibrated & isotropic 3D images at micron resolutions
- Covers a very large range of sample sizes
- Gives information at different length scales
- Nondestructive imaging, thus compatible with routine sample preparation.
  Enables correlative imaging pipelines, scanning of museum & collection material

Biomedical imaging

- Medical research
- Non-destructive insights into the samples
- (Small) Biological samples

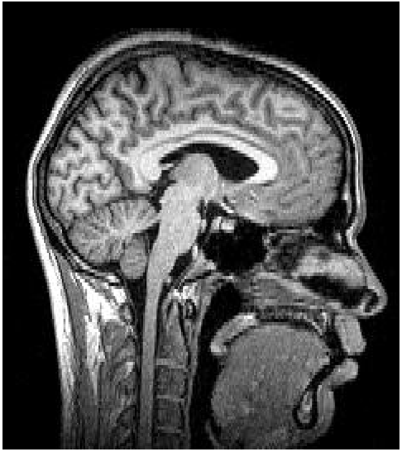

Biomedical imaging

- Medical research
- Non-destructive i
- (Small) Biologica

Biomedical imaging

- Medical research
- Non-destructive insights into the samples
- (Small) Biological samples

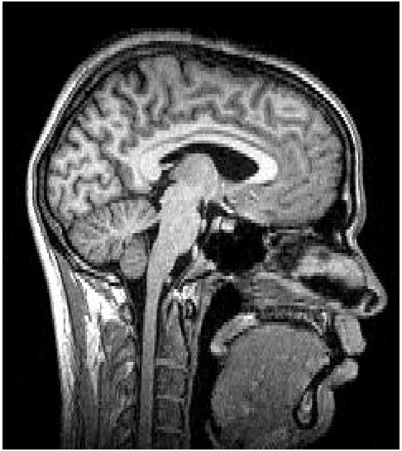

w.wiki/7g4

Biomedical imaging

- Medical research
- Non-destructive i
- (Small) Biologica

Wavelengths & Scales

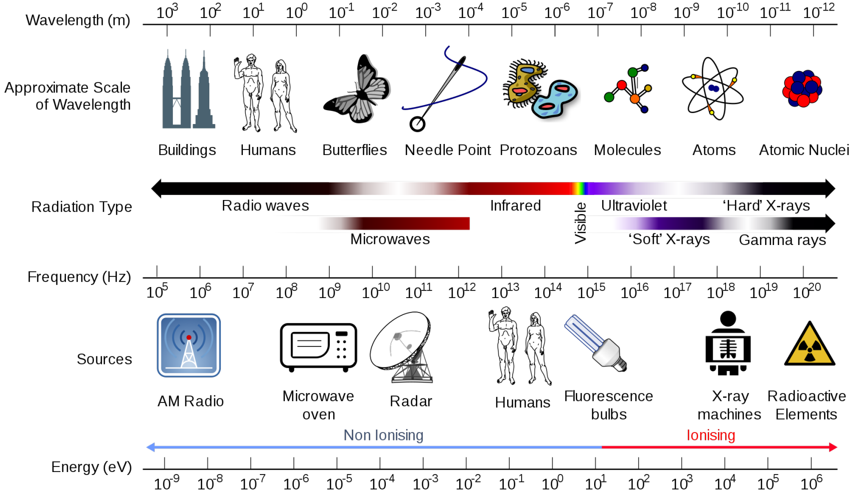

Wavelengths & Scales

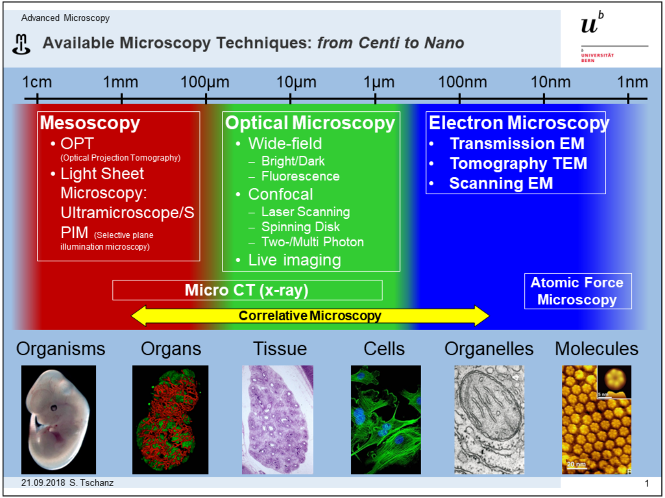

Stefan Tschanz, with permission

Wavelengths & Scales

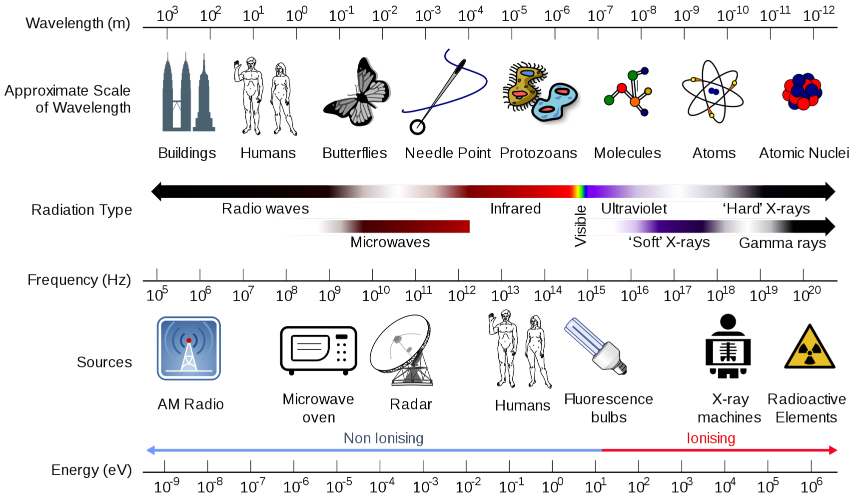

Wavelengths & Scales

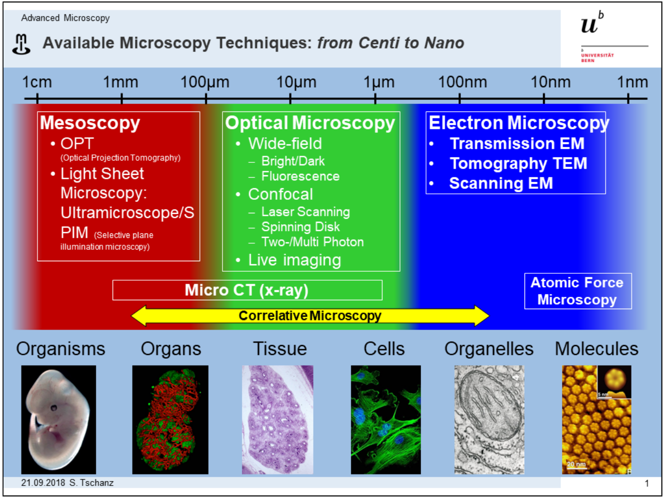

Stefan Tschanz, with permission

Imaging methods

- Light (sheet) microscopy: see lecture of Nadia Mercader Huber
- X-ray imaging
- Electron microscopy
  - *Analytical electron microscopy* by Dimitri
  - *SEM Grundlagen* by Sabine Kässmeyer and Ivana Jaric
  - *Cryoelectron Microscopy & Serial Block Face SEM* by Ioan

Imaging methods

- Light (sheet) microscopy: see lecture of Nadia Mercader Huber
- X-ray imaging
- Electron microscopy
  - *Analytical electron microscopy* by Dimitri
  - *SEM Grundlagen* by Sabine Kässmeyer and Ivana Jaric
  - *Cryoelectron Microscopy & Serial Block Face SEM* by Ioan

CT-Scanner

youtu.be/2CWpZKuy-NE

CT-Scanner

youtu.be/2CWpZKuy-NE

CT History

- 1895: Wilhelm Conrad Röntgen discovers X-rays

w.wiki/BHAN

CT History

- 1895: Wilhelm Conrad Röntgen discovers X-rays
- 1963: Cormack used a collimated ^{60}Co source and a Geiger counter as a detector [12]
- 1976: Hounsfield worked on first clinical scanner [13]

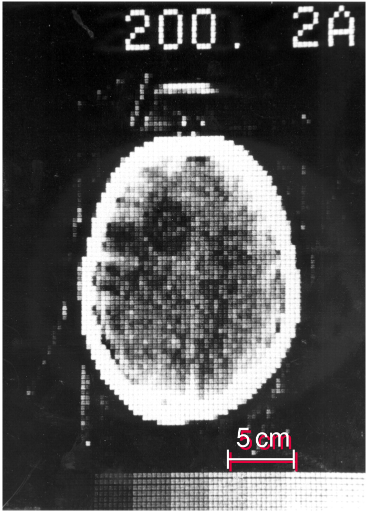

From [14], Figure 5

CT History

- 1895: Wilhelm Conrad Röntgen discovers X-rays
- 1963: Cormack used a collimated ^{60}Co source and a Geiger counter as a detector [12]
- 1976: Hounsfield worked on first clinical scanner [13]
- CT scanner generations
  - First generation

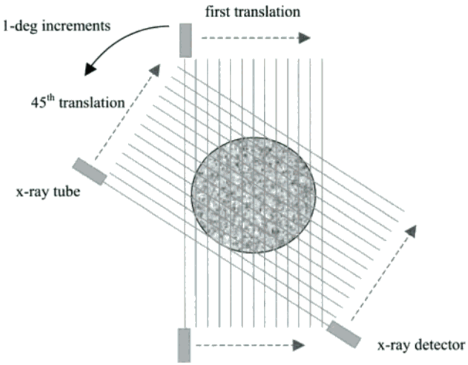

From [15], Figure 1.12

CT History

- 1895: Wilhelm Conrad Röntgen discovers X-rays
- 1963: Cormack used a collimated ^{60}Co source and a Geiger counter as a detector [12]
- 1976: Hounsfield worked on first clinical scanner [13]
- CT scanner generations
  - First generation
  - Second generation

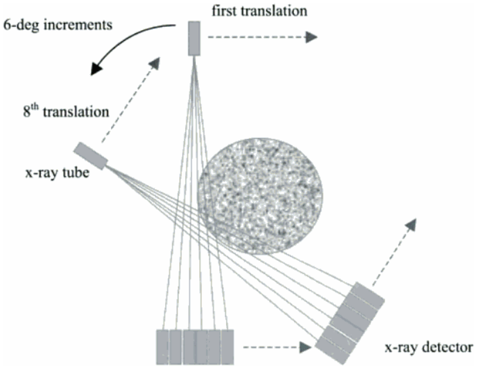

From [15], Figure 1.13

CT History

- 1895: Wilhelm Conrad Röntgen discovers X-rays
- 1963: Cormack used a collimated ^{60}Co source and a Geiger counter as a detector [12]
- 1976: Hounsfield worked on first clinical scanner [13]
- CT scanner generations
  - First generation
  - Second generation
  - Third generation

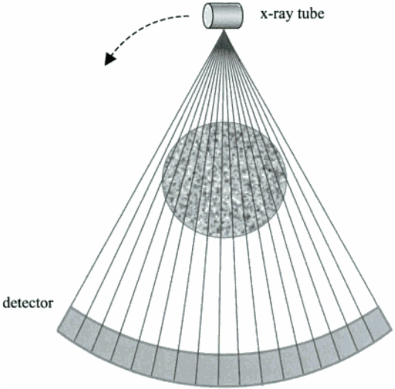

From [15], Figure 1.14

µCT History I

- X-ray computed tomography began to replace analog focal plane tomography in the early 1970s [16]
- In the early 1980s, Lee Feldkamp [17] developed one of the early laboratory microCT systems by assembling a micro-focus cone beam x-ray source, specimen holder and stagers, and an image intensifier at Ford Motor Company's Scientific Research Laboratory to nondestructively detect damage in ceramic manufactured automobile parts
- Met with scientists at Henry Ford Hospital and University of Michigan interested in understanding bone microstructure [18] and osteoarthritis [19]
- 1987: The first commercially available µCT scanner was developed by SkyScan (now Bruker)

μCT History II

- Today: μCT is widely used in various fields for non-destructive imaging
  - quantifying the microstructure of organic materials, particularly mineralized bone tissue and the relationships between the mechanical behavior of bone to its structural and compositional properties
  - Material Science: internal structure of composites, foams, and other materials. Understand the relationship between structure and properties.
  - Biomedical Research: microarchitecture of bone tissue, dental research, and small animal imaging. Since the 1990s, μCT includes imaging of soft tissues and vasculature using radio-opaque contrast agents
  - Paleontology and Archaeology: study of fossils and archaeological artifacts
- $\approx$2500 μCT systems are in use worldwide with over 1000 publications annually

µCT History I

- X-ray computed tomography began to replace analog focal plane tomography in the early 1970s [16]
- In the early 1980s, Lee Feldkamp [17] developed one of the early laboratory microCT systems by assembling a micro-focus cone beam x-ray source, specimen holder and stagers, and an image intensifier at Ford Motor Company's Scientific Research Laboratory to nondestructively detect damage in ceramic manufactured automobile parts
- Met with scientists at Henry Ford Hospital and University of Michigan interested in understanding bone microstructure [18] and osteoarthritis [19]
- 1987: The first commercially available µCT scanner was developed by SkyScan (now Bruker)

µCT History II

- Today: µCT is widely used in various fields for non-destructive imaging
  - quantifying the microstructure of organic materials, particularly mineralized bone tissue and the relationships between the mechanical behavior of bone to its structural and compositional properties
  - Material Science: internal structure of composites, foams, and other materials. Understand the relationship between structure and properties.
  - Biomedical Research: microarchitecture of bone tissue, dental research, and small animal imaging. Since the 1990s, µCT includes imaging of soft tissues and vasculature using radio-opaque contrast agents
  - Paleontology and Archaeology: study of fossils and archaeological artifacts
- $\approx$2500 µCT systems are in use worldwide with over 1000 publications annually

X-ray interaction

- "X-rays interact with tissue in 2 main ways: photoelectric effect and Compton scatter. To a first approximation, the photoelectric effect contributes to contrast while the Compton effect contributes to noise. Both contribute to dose." ([20])
  - Photoelectric absorption (τ) is strongly dependent on the atomic number Z of the absorbing material: $\tau \propto \frac{Z^4}{E^{3.5}}$
  - Compton scattering is one of the principle forms of photon interaction and is directly proportional to the (electron & physical) density of the material. It does *not* depend on the atomic number: $\lambda' - \lambda = \frac{h}{m_e c}(1 - \cos\theta)$
- Lowering x-ray energy increases contrast
- X-ray penetration decreases exponentially with sample thickness [21, i. e. Beer-Lamberts law]: $I(t) = I_0\, e^{-\alpha z}$

Composition of biological tissues

Tissue: content by mass percentage

Element Atomic number	H 1	C 6	N 7	O 8	Na 11	P 15	S 16	Cl 17	K 19	Ca 20
Fat	11.4	59.8	0.7	27.8	0.1		0.1	0.1		
Water	11.2			88.8						
Blood	10.2	11	3.3	74.5	0.1	0.1	0.2	0.3	0.2	
Liver	10.2	13.9	3	71.6	0.3	0.2	0.3	0.2	0.3	
Brain	10.7	14.5	2.2	71.2	0.2	0.4	0.2	0.3	0.3	
Bone	3.4	15.5	4.2	43.5	0.1	10.3	0.3			22.5

Why µCT?

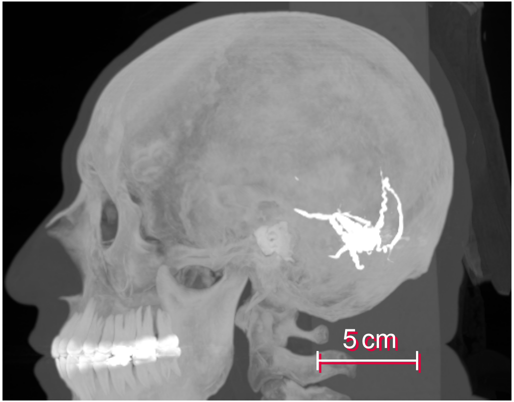

From [22], Subject *C3L-02465*

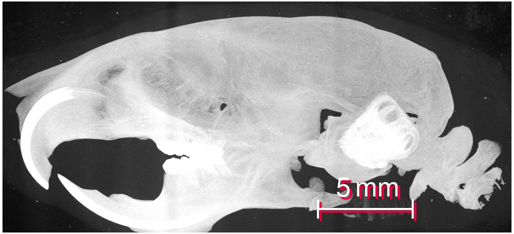

Why µCT?

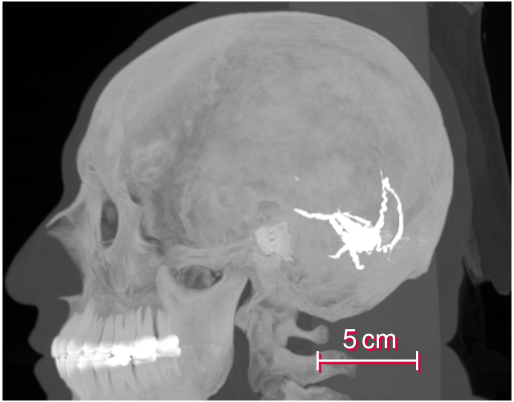

From [22], Subject *C3L-02465*

Why µCT?

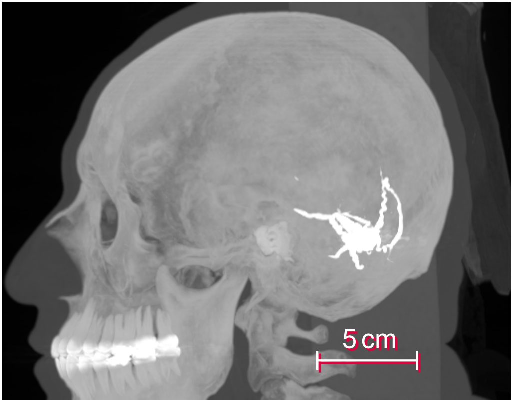

From [22], Subject *C3L-02465*

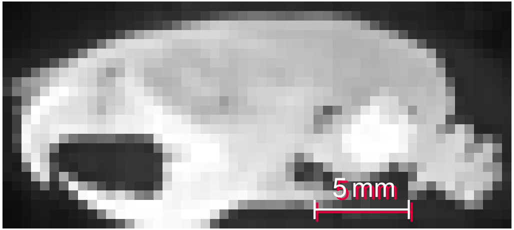

Why µCT?

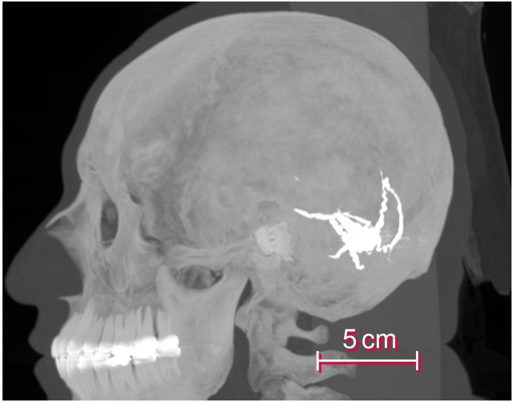

From [22], Subject *C3L-02465*

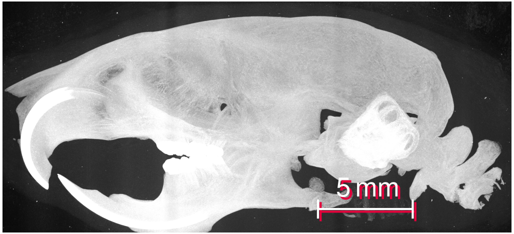

Why µCT?

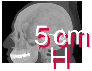

From [22], Subject *C3L-02465*

Maximum intensity projection

Projections

Reducing the dimensions of a dataset. For example projecting a volume (3D) to a surface by taking the maximum value across planes for each pixel.

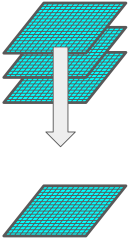

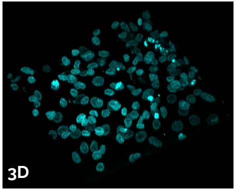

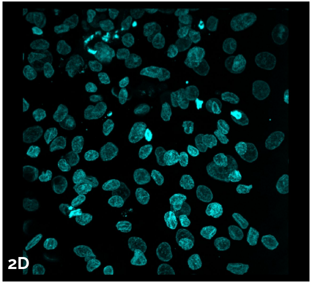

Fundamentals of Digital Image Processing (2022) by Guillaume Witz, Slide 23

Machinery

- Hospital CT
  - Voxel size around 0.5 mm
- Lab/Desktop CT
  - Voxel size around 7 µm (*in vivo*) or 0.5 µm (*ex vivo*)
- Synchrotron CT
  - Voxel size down to 160 nm

trim=<left> <lower> <right> <upper>

flic.kr/p/D4rbom

Machinery

- Hospital CT
  - Voxel size around 0.5 mm
- Lab/Desktop CT
  - Voxel size around 7 µm (*in vivo*) or 0.5 µm (*ex vivo*)
- Synchrotron CT
  - Voxel size down to 160 nm

trim=<left> <lower> <right> <upper>

Machinery

- Hospital CT
  - Voxel size around 0.5 mm
- Lab/Desktop CT
  - Voxel size around 7 µm (*in vivo*) or 0.5 µm (*ex vivo*)
- Synchrotron CT
  - Voxel size down to 160 nm

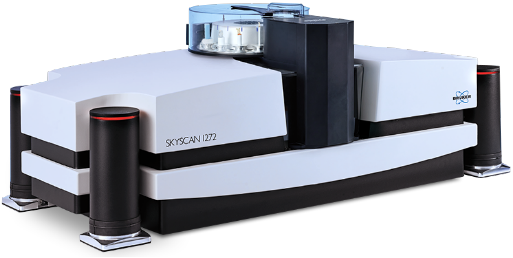

trim=<left> <lower> <right> <upper>

bruker.com/skyscan1272

Machinery

- Hospital CT
  - Voxel size around 0.5 mm
- Lab/Desktop CT
  - Voxel size around 7 µm (*in vivo*) or 0.5 µm (*ex vivo*)
- Synchrotron CT
  - Voxel size down to 160 nm

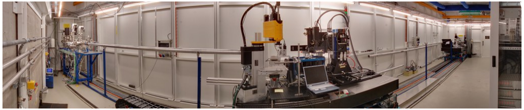

trim=<left> <lower> <right> <upper>

flic.kr/p/7Xhk2Y

What is happening?

No matter what kind of machine, the basic principle is always the same

- an x-ray source
- a sample
- a detector

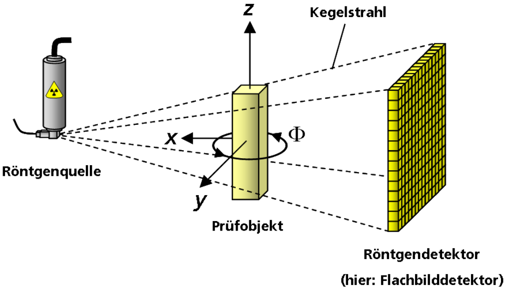

Machinery

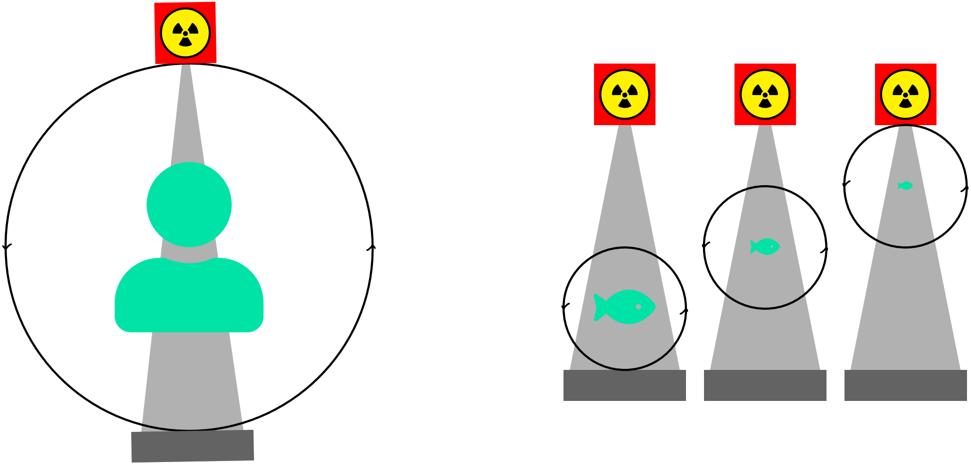

Examples

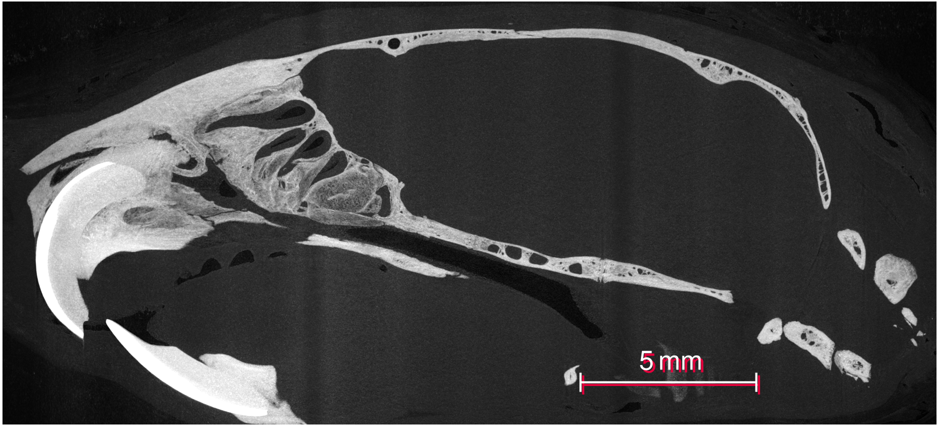

Examples

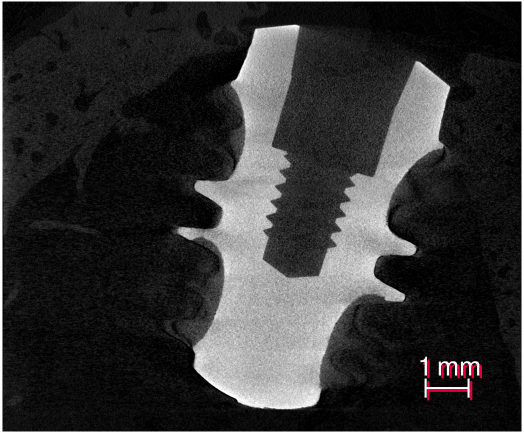

Examples

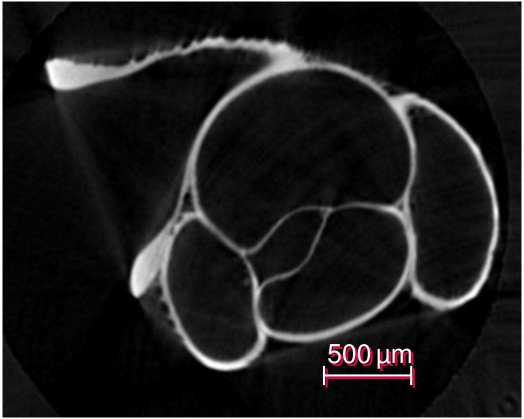

From [8], *Diancta phoenīx*

Examples

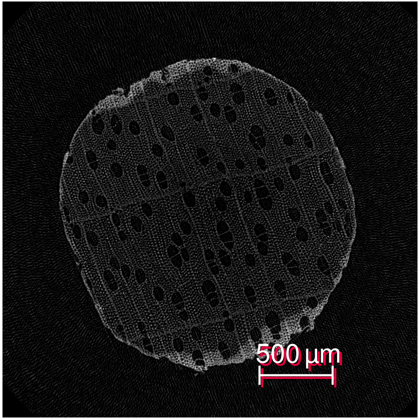

Examples

Preparation

- Study design
- Sample preparation

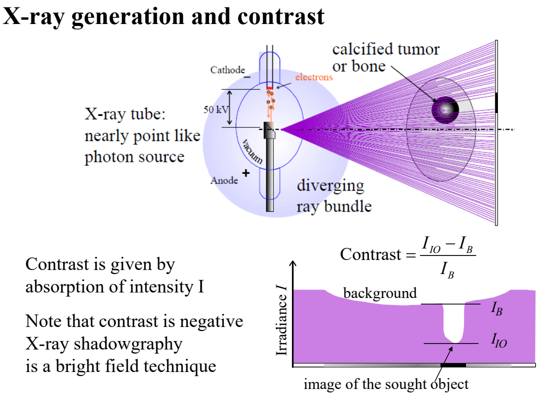

Contrast, Magnification and Resolution—Laws of Physics for Microscopists (1, 2022) by Martin Frenz, Slide 21

Projection acquisition

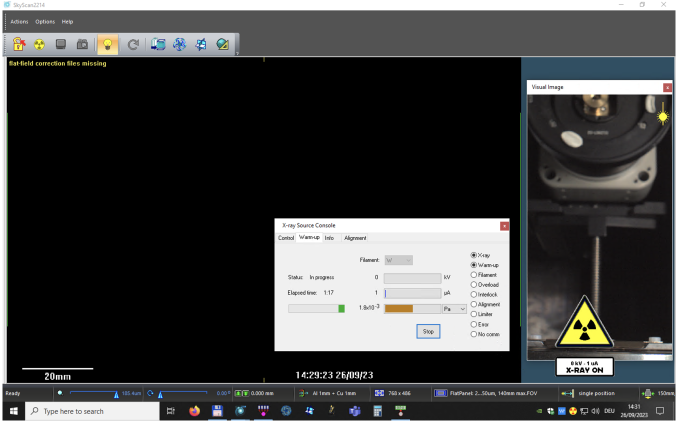

Projections

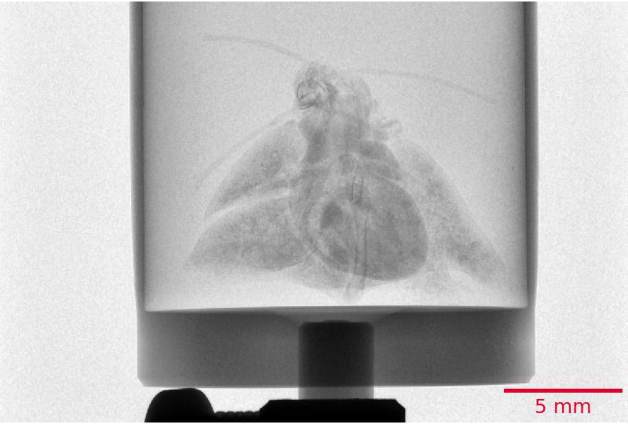

Projections

- A (micro-focus) x-ray source illuminates the object
- The x-rays penetrate the sample and are attenuated
- A scintillator converts the x-rays to visible light
- A (planar) x-ray detector collects (magnified) projection images.
- The projections are recorded on disk

Reconstructions

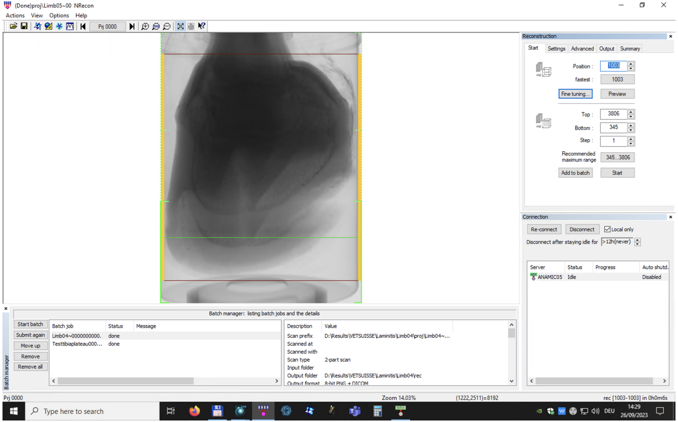

Reconstructions

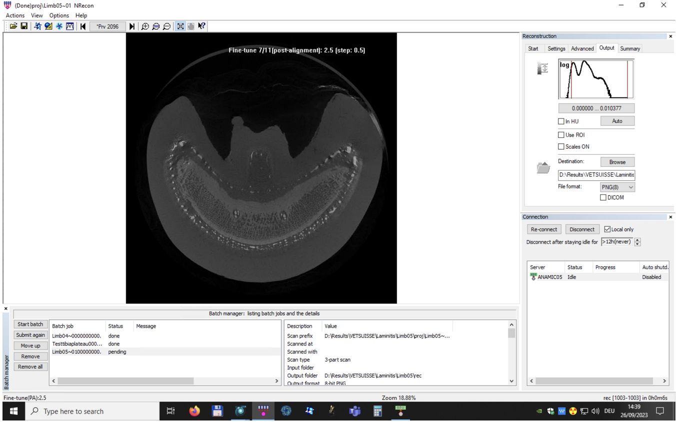

Reconstructions

Reconstructions

- Based on hundreds of angular views acquired while the object rotates, a computer synthesizes a stack of virtual cross section slices through the object.
- Radon Transformation
- Filtered back projection
- Fan beam reconstruction
- Corrections (beam hardening, etc.)
- Writing to stack

Visualization

Visualization

- Based the on reconstructions, a computer synthesizes a three-dimensional view of the scanned sample

What to use?

- ImageJ/Fiji [23]
- Also see *Fundamentals of Digital Image Processing* by Guillaume Witz
- Reproducible research
  - in Jupyter [24]
  - **git**
  - Script all your things!
  - Data repositories; i. e. sharing is caring!

Quantitative data

- Pretty images are nice, but we need quantitative numbers
- Segmentation
- Characterization

Internal morphology of human teeth

Collaboration with zmk bern – Zahnmedizinische Kliniken

- Numbers instead of just pretty images
- Segm
- (

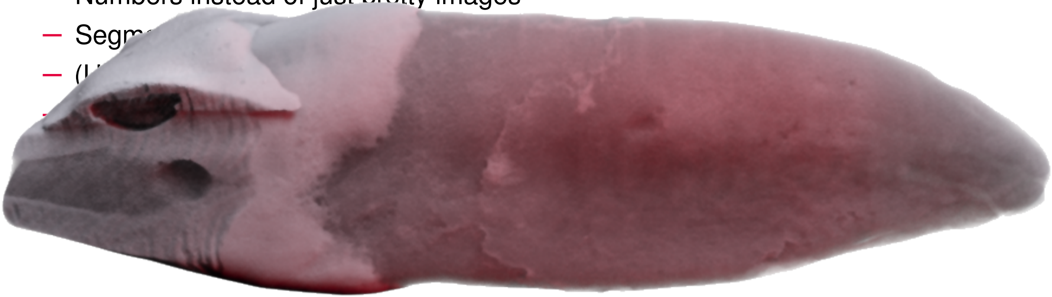

Internal morphology of human teeth

Collaboration with zmk bern – Zahnmedizinische Kliniken

- Numbers instead of just pretty images
- Segmentation of teeth and root canal
- (Unbiased) Characterization
- Reproducible and automated image analysis (in Jupyter [24])
- Two publications:
  - [10], BMC Oral Health, doi.org/gjpw2d
  - [25], Scientific Reports, doi.org/g7r8

How?

- 104 extracted human permanent mandibular canines
- µCT imaging
- Root canal configuration, according to Briseño-Marroquín *et al.* [26]
- *Reproducible* analysis [27], e. g. you can click a button to double-check or recalculate the results yourself!

How?

- 104 extracted human permanent mandibular canines
- µCT imaging
- Root canal configuration, according to Briseño-Marroquín *et al.* [26]
- *Reproducible* analysis [27], e. g. you can click a button to double-check or recalculate the results yourself!

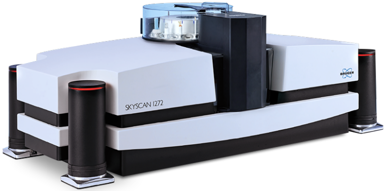

bruker.com/skyscan1272

How?

- 104 extracted human permanent mandibular canines
- µCT imaging
- Root canal configuration, according to Briseño-Marroquín *et al.* [26]
- *Reproducible* analysis [27], e. g. you can click a button to double-check or recalculate the results yourself!

```
Scanner=SkyScan1272
Instrument S/N=15G09089-B
Software Version=1.1.19
Filename Prefix=Tooth045~00
Number Of Files=  482
Number Of Rows= 1092
Number Of Columns= 1632
Source Voltage (kV)=  80
Source Current (uA)= 125
Image Pixel Size (um)=9.999986
Exposure (ms)=950
Rotation Step (deg)=0.400
Frame Averaging=ON (3)
Filter=Al 1mm
Study Date and Time=02 Jul 2020  08h:23m:34s
Scan duration=0h:39m:51s
```

How?

- 104 extracted human permanent mandibular canines
- µCT imaging
- Root canal configuration, according to Briseño-Marroquín *et al.* [26]
- *Reproducible* analysis [27], e. g. you can click a button to double-check or recalculate the results yourself!

Sample changer on the SkyScan 1272
In total:

- 13 days of *continuous* µCT scanning
- 819 GB of raw data
  230 648 TIFF projections
- 326 GB data as input for analysis
  282 062 PNG reconstructions

How?

- 104 extracted human permanent mandibular canines
- µCT imaging
- Root canal configuration, according to Briseño-Marroquín *et al.* [26]
- *Reproducible* analysis [27], e. g. you can click a button to double-check or recalculate the results yourself!

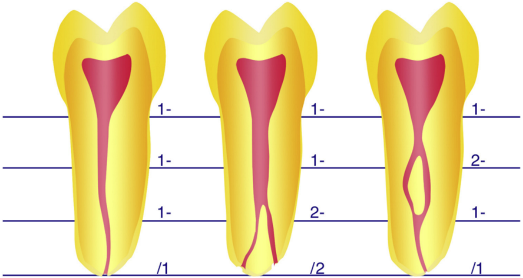

From [26], Fig. 2

How?

- 104 extracted human permanent mandibular canines
- µCT imaging
- Root canal configuration, according to Briseño-Marroquín *et al.* [26]
- *Reproducible* analysis [27], e. g. you can click a button to double-check or recalculate the results yourself!

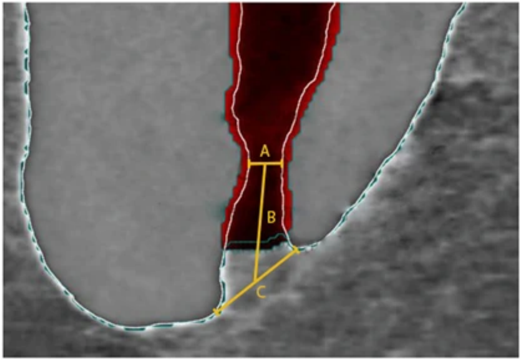

From [28], Fig. 1

How?

- 104 extracted human permanent mandibular canines
- µCT imaging
- Root canal configuration, according to Briseño-Marroquín *et al.* [26]
- *Reproducible* analysis [27], e. g. you can click a button to double-check or recalculate the results yourself!

gph.is/2nqkple

How?

- 104 extracted human permanent mandibular canines
- µCT imaging
- Root canal configuration, according to Briseño-Marroquín *et al.* [26]
- *Reproducible* analysis [27], e. g. you can click a button to double-check or recalculate the results yourself!

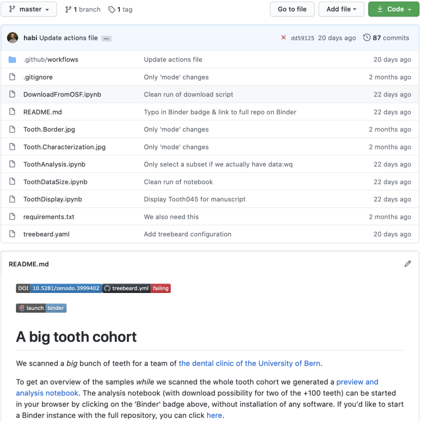

µCT imaging

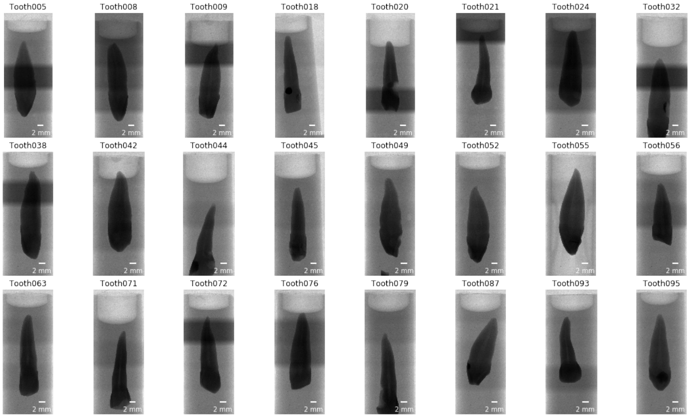

Tooth005
2 mm
Tooth008
2 mm
Tooth009
2 mm
Tooth018
2 mm
Tooth020
2 mm
Tooth021
2 mm
Tooth024
2 mm
Tooth032
2 mm
Tooth038
2 mm
Tooth042
2 mm
Tooth044
2 mm
Tooth045
2 mm
Tooth049
2 mm
Tooth052
2 mm
Tooth055
2 mm
Tooth056
2 mm
Tooth063
2 mm
Tooth071
2 mm
Tooth072
2 mm
Tooth076
2 mm
Tooth079
2 mm
Tooth087
2 mm
Tooth093
2 mm
Tooth095
2 mm

Dataset cropping

- Full datasets: 326 GB
- Cropped datasets: 115 GB

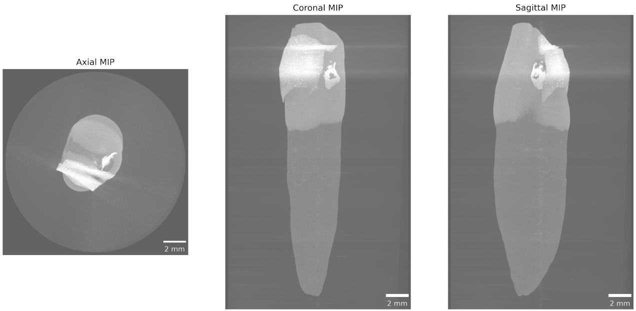

Dataset cropping

- Full datasets: 326 GB
- Cropped datasets: 115 GB

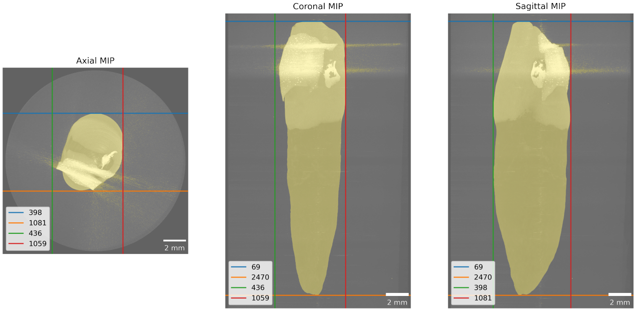

Tooth morphology

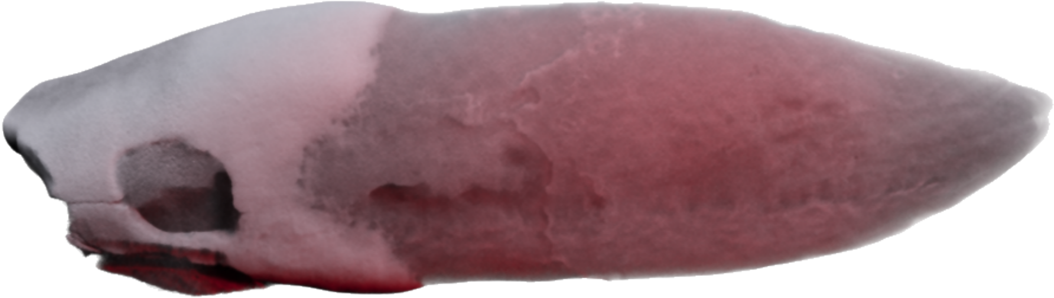

Tooth morphology

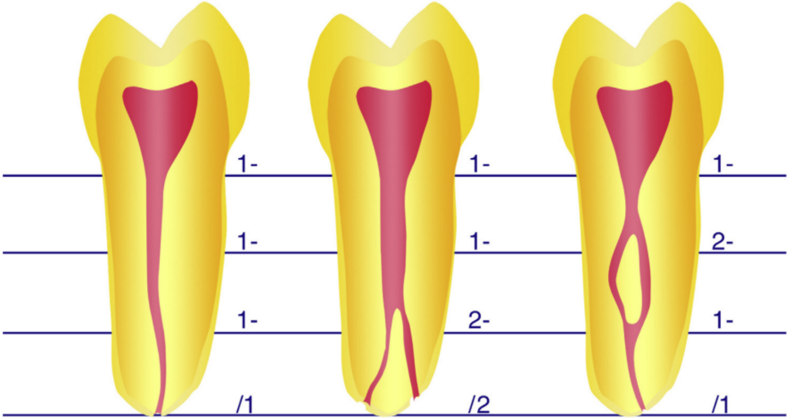

From [26], Fig. 2

Tooth morphology

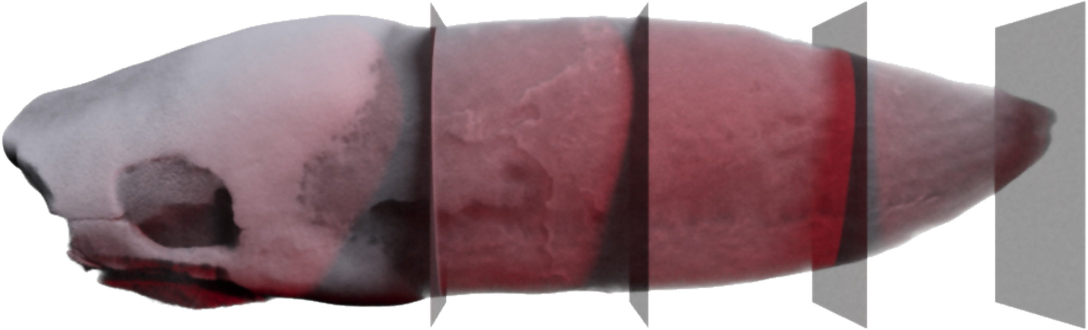

Detection of enamel-dentin border

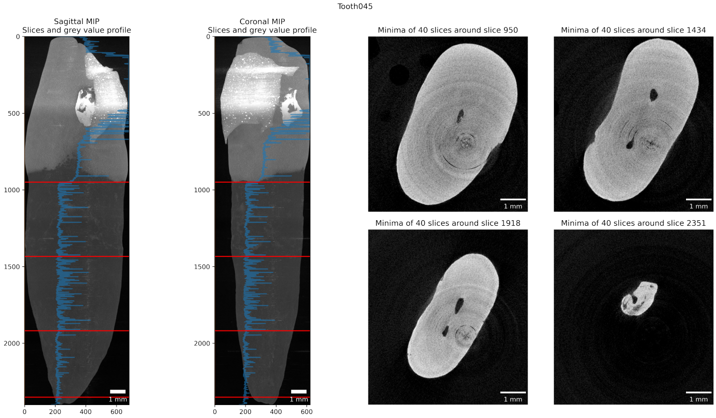

Detection of enamel-dentin border

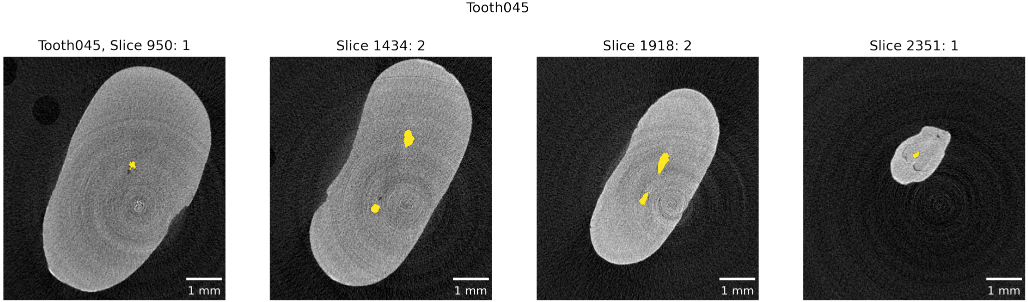

Outcome root canal configuration classification

Roots		RCC	#	%
Single (N=98)		1-1-1/1	73	74.5
		1-1-1/2	14	14.3
		1-1-1/3	1	1.0
		1-1-1/4	2	2.1
		1-1-2/1	1	1.0
		1-2-1/1	4	4.1
		1-2-1/2	1	1.0
		1-2-2/2	1	1.0
		2-3-1/1	1	1.0
Double (N=3)	Buccal	1-1-1/1	2	66.6
		1-2-1/1	1	33.3
	Lingual	1-1-1/1	2	66.6
		1-1-1/2	1	33.3

Extraction of root canal space

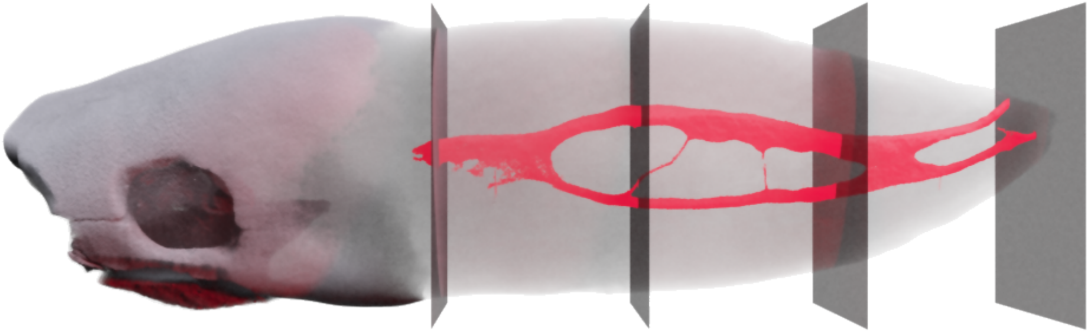

Results of root canal space extraction

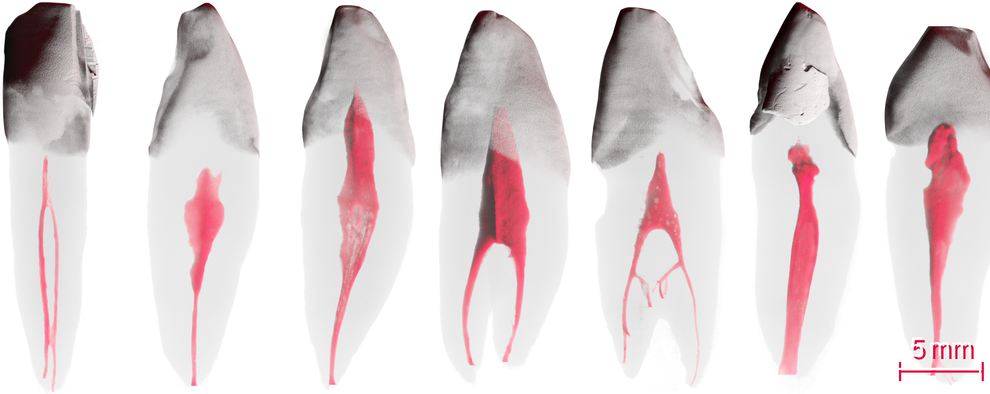

Analysis of the physiological foramen geometry

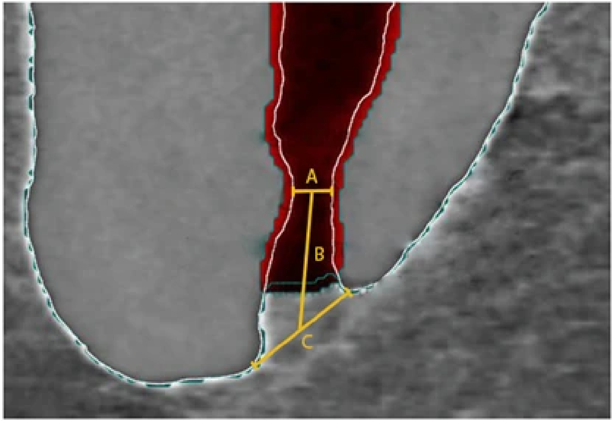

From [28], Fig. 1

Analysis of the physiological foramen geometry

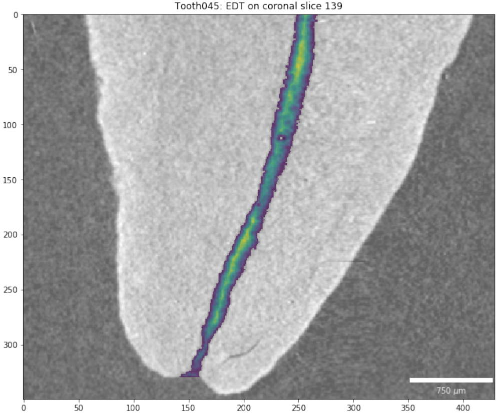

Conclusion ZMK

- Efficient use of time, e. g. more teeth does not mean more (human) work
- Reproducible analysis with *free and open-source* software, usable by *anyone*
- Objective analysis, e. g. no operator bias

Metal foam

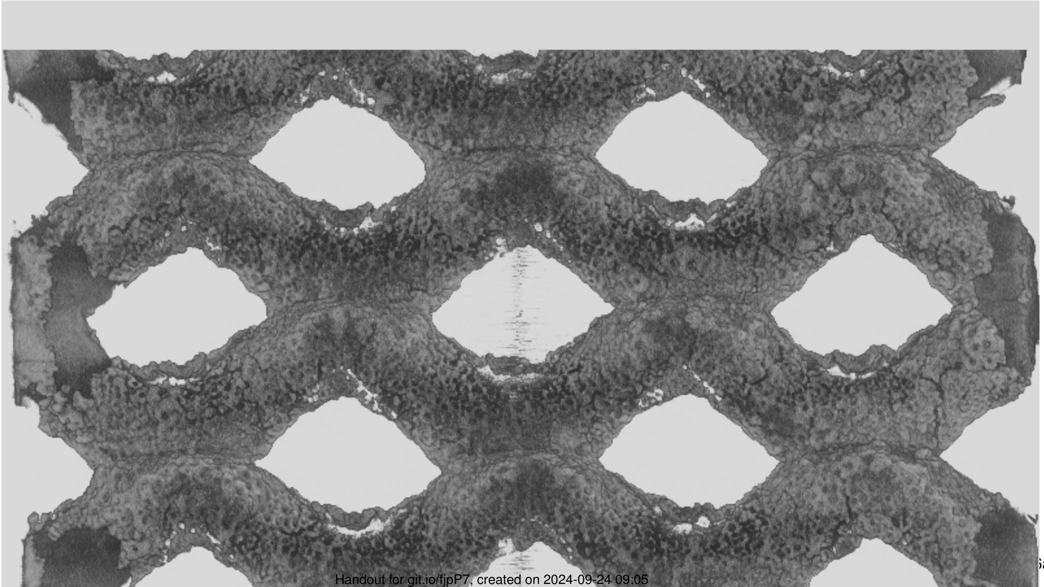

Data wrangling by example: Cichlids

Collaboration with team of *Aquatic Ecology & Evolution*, from the Institute of Ecology and Evolution [11]

- 133 Cichlids from Lake Victoria, East Africa
  - Functional anatomy of the skulls and jaws
  - 6–18 cm in size
- 375 scans in total
  - Voxelsizes from 3.5–50 µm
  - 46 days of scanning time
  - 9.8 TB of raw data
  - 1.5 TB/+1 000 000 reconstructions

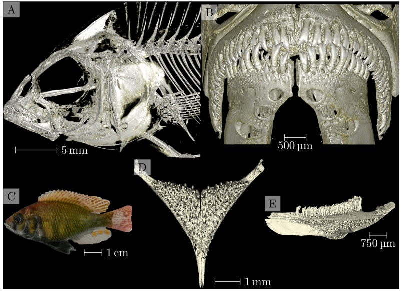

DOI:gsst8t, Fig. 1

[11] D. Haberthür *et al.*, Sep. 2023. DOI: gsst8t.

Visualization of cichlid head

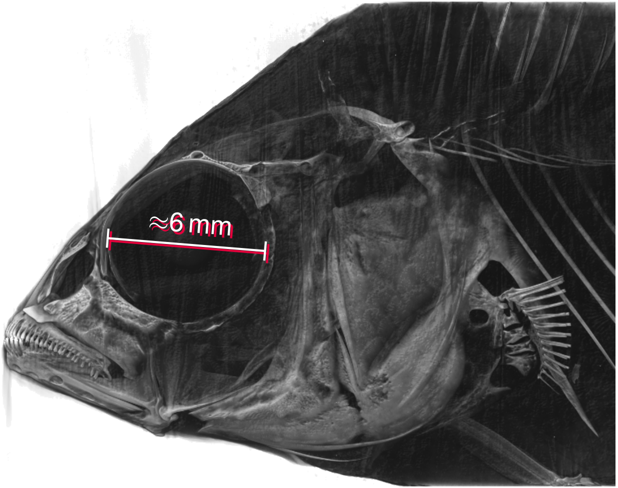

Visualization of cichlid head

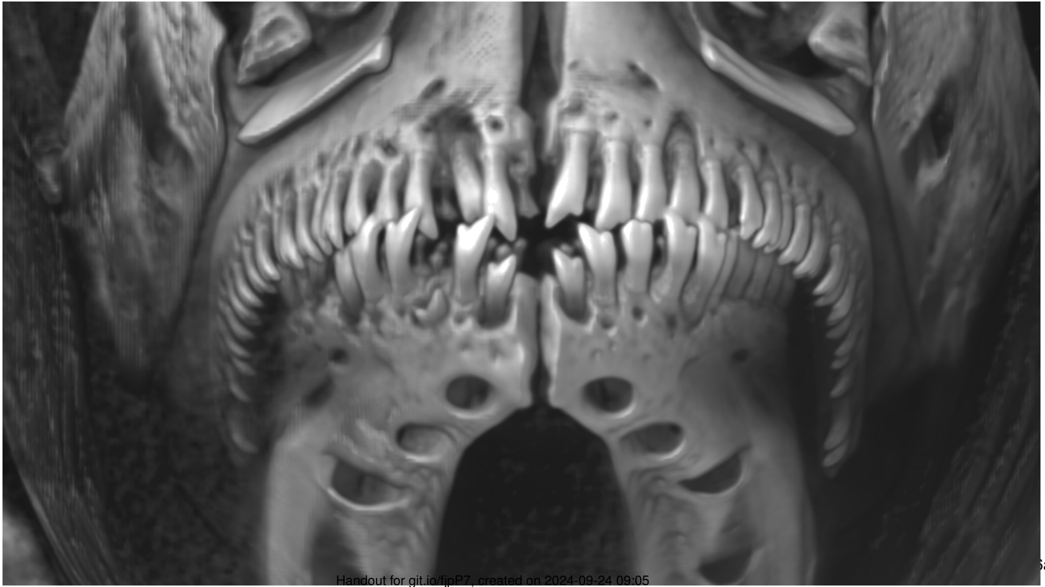

Visualization of segmented pharyngeal jaw

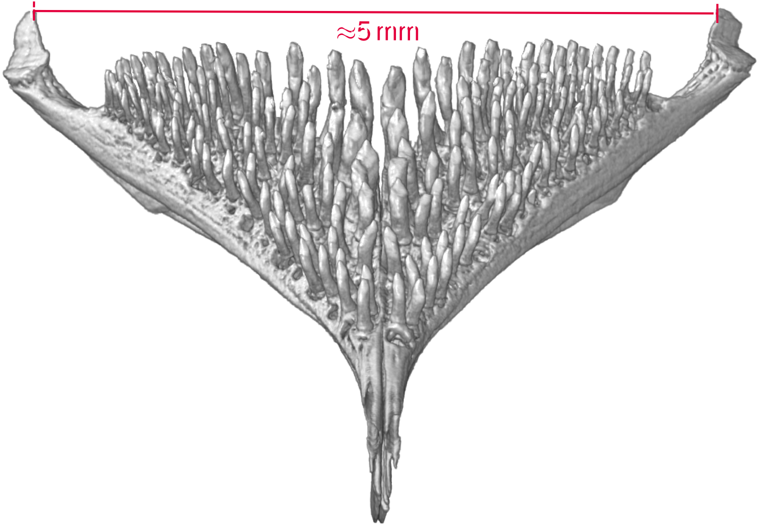

Data wrangling by example: Cichlids

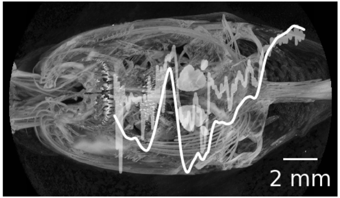

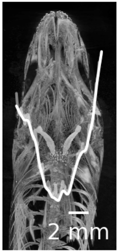

Data wrangling by example: Cichlids

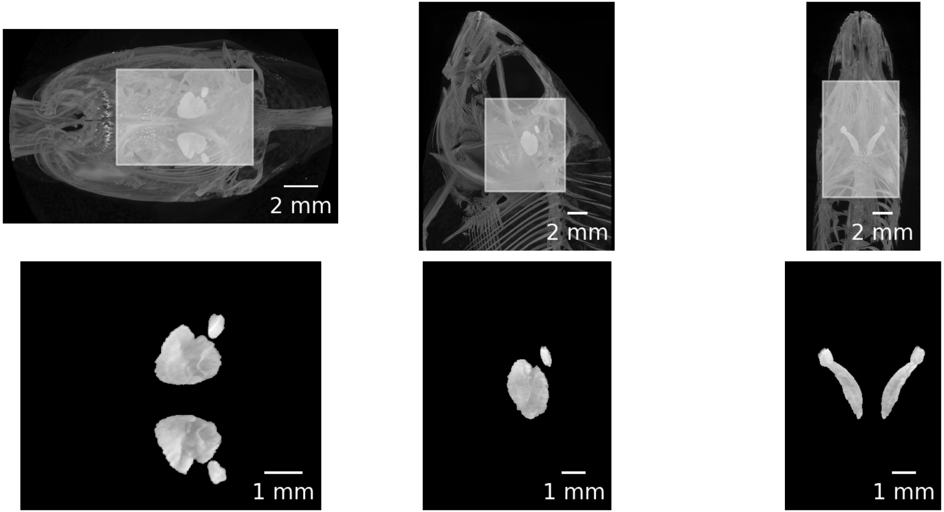

Thanks!

- Thanks for listening to me!
- What questions do you have for me?

Colophon

- This BEAMER presentation was crafted in LaTeX with the (slightly adapted) template from *Corporate Design und Vorlagen* of the University of Bern.
  - Complete source code: git.io/fjpP7
  - The LaTeX code is automatically compiled with a GitHub action to a (handout) PDF which you can access here: git.io/JeQxO
- Did you spot an error?
  - File an issue: git.io/fjpPb
  - Submit a pull request: git.io/fjpPN
  - Send me an email: david.haberthuer@unibe.ch

References I

[1] R. Hlushchuk *et al.*, “Cutting-edge microangio-CT: New dimensions in vascular imaging and kidney morphometry,”, Mar. 2018. DOI: 10.1152/ajprenal.00099.2017.

[2] H. Nording *et al.*, “The C5a/C5a receptor 1 axis controls tissue neovascularization through CXCL4 release from platelets,”, Dec. 2021. DOI: 10.1038/s41467-021-23499-w.

[3] R. Hlushchuk *et al.*, “Innovative high-resolution microCT imaging of animal brain vasculature,”, Oct. 2020. DOI: 10.1007/s00429-020-02158-8.

[4] T. Wüthrich *et al.*, “Development of vascularized nerve scaffold using perfusion-decellularization and recellularization,”, Aug. 2020. DOI: 10.1016/j.msec.2020.111311.

[5] C. Zubler *et al.*, “The anatomical reliability of the superficial circumflex iliac artery perforator (SCIP) flap,”, Mar. 2021. DOI: 10.1016/j.aanat.2020.151624.

[6] M. Messerli *et al.*, “Adaptation mechanism of the adult zebrafish respiratory organ to endurance training,”, Feb. 2020. DOI: 10.1371/journal.pone.0228333.

[7] V. Trappetti *et al.*, “Synchrotron Microbeam Radiotherapy for the treatment of lung carcinoma: A pre-clinical study,”, Aug. 2021. DOI: 10.1016/j.ijrobp.2021.07.1717.

[8] E. Bochud *et al.*, “A new Diancta species of the family Diplommatinidae (Cyclophoroidea) from Vanua Levu Island, Fiji,”, Nov. 2021. DOI: 10.3897/zookeys.1073.73241.

[9] S. Halm *et al.*, “Micro-CT imaging of Thiel-embalmed and iodine-stained human temporal bone for 3D modeling,”, 2021. DOI: 10.1186/s40463-021-00522-0.

[10] D. Haberthür *et al.*, “Automated segmentation and description of the internal morphology of human permanent teeth by means of micro-CT,”, Apr. 2021. DOI: gjpw2d.

References II

[11] D. Haberthür *et al.*, “Microtomographic investigation of a large corpus of cichlids,”, Sep. 2023. DOI: gsst8t.

[12] A. M. Cormack., “Representation of a Function by Its Line Integrals, with Some Radiological Applications,”, Sep. 1963. DOI: 10.1063/1.1729798.

[13] G. N. Hounsfield., “Historical notes on computerized axial tomography.,”, 1976.

[14] E. C. Beckmann., “CT scanning the early days.,”, Jan. 2006. DOI: 10.1259/bjr/29444122.

[15] J. Hsieh. *Computed Tomography: Principles, Design, Artifacts, and Recent Advances*. Society of Photo Optical, 2003.

[16] A. S. Lin *et al.* “Microcomputed Tomography,” in *Springer Handbook of Microscopy*, ser. Springer Handbooks, Cham: Springer International Publishing, 2019. DOI: 10.1007/978-3-030-00069-1_24.

[17] L. A. Feldkamp *et al.*, “Practical cone-beam algorithm,”, Jun. 1984. DOI: 10.1364/JOSAA.1.000612.

[18] L. A. Feldkamp *et al.*, “The direct examination of three-dimensional bone architecture in vitro by computed tomography,”, Feb. 1989. DOI: 10.1002/jbmr.5650040103.

[19] M. W. Layton *et al.*, “Examination of subchondral bone architecture in experimental osteoarthritis by microscopic computed axial tomography,”, Nov. 1988. DOI: 10.1002/art.1780311109.

[20] M. Hammer. *X-Ray Physics: X-Ray Interaction with Matter, X-Ray Contrast, and Dose*, http://xrayphysics.com/attenuation.html.

[21] Wikipedia contributors. *Beer–Lambert law — Wikipedia, The Free Encyclopedia*, 2019.

[22] K. Clark *et al.*, “The Cancer Imaging Archive (TCIA): Maintaining and Operating a Public Information Repository,”, Dec. 2013. DOI: 10.1007/s10278-013-9622-7.

References III

[23] J. Schindelin *et al.*, "Fiji: An open-source platform for biological-image analysis,", Jul. 2012. DOI: 10.1038/nmeth.2019.

[24] T. Kluyver *et al.*, "Jupyter Notebooks – a publishing format for reproducible computational workflows,", 2016. DOI: 10.3233/978-1-61499-649-1-87.

[25] T. G. Wolf *et al.*, "Internal morphology of 101 mandibular canines of a Swiss-German population by means of micro-CT: An ex vivo study,", 2021. DOI: g7r8.

[26] B. Briseño-Marroquín *et al.*, "Root Canal Morphology and Configuration of 179 Maxillary First Molars by Means of Micro–computed Tomography: An Ex Vivo Study,", Dec. 2015. DOI: 10.1016/j.joen.2015.09.007.

[27] D. Haberthür., "Habi/zmk-tooth-cohort: Used for manuscript about method,", Aug. 2020. DOI: 10.5281/ZENODO.3999402.

[28] T. G. Wolf *et al.*, "Three-dimensional analysis of the physiological foramen geometry of maxillary and mandibular molars by means of micro-CT,", Sep. 2017. DOI: 10.1038/ijos.2017.29.